Open Access Journal
Journal of Power Technologies 93 (1) (2013) 27–36
journal homepage:papers.itc.pw.edu.pl

Electrochemical model for proton exchange membrane fuel cell systems

Abdellah Beicha*,[a], Radia Zaamouche[b]

[a] *Jijel University, Faculty of Sciences and Technology*
Department of Process Engineering 18000 Jijel, Algeria
[b] *University of Batna, Faculty of Sciences and Technology*
Department of Mechanics 05000 Batna, Algeria

Abstract

This paper presents an electrochemical model for simulation and evaluation of the performance of a proton exchange membrane (PEM) fuel cell. The results of the model are used to predict the efficiency and power of the fuel cell as a function of operational parameters of the cell, like temperature, partial pressures and membrane humidity. A one-dimensional mass transport model was also developed to investigate water transport through the membrane electrode assembly (MEA). The model enables quantification of the water flux corresponding to each of the three water transport mechanisms, such as diffusion, electro-osmotic drag and convection. The influence of temperature on the fuel cell's characteristics is more pronounced than the influence of partial pressures and membrane humidity. The effect of platinum loading on cell performance is examined with Pt loadings of 0.18, 0.38 and 0.4 mg/cm^2.

Keywords: Fuel cell, Modeling, Simulation, Power, Membrane

1. Introduction

Non-polluting energy generation and other environmental issues have been driving an increasing demand over the last few years for new energy conversion technologies. It is in this context that PEM fuel cell systems constitute a promising alternative due their high efficiency and low impact on the environment. A theoretical approach with mathematical simulation is very effective for designing and analyzing the performance of the PEM fuel cell.

Some work has been reported in the literature on steady-state fuel-cell modeling (e.g. [1–4], as well as dynamic modeling [5–7]). These studies are mostly based on empirical equations and/or the electrochemical reactions inside the fuel cell. Also there are several studies regarding the influence of certain operating parameters on fuel cell characteristics [8]. Many other models have been developed and reported in literature, but they did not focus on the impact of individual operating parameters on fuel cell output characteristics.

This paper presents a simple model of a PEM fuel cell that can be used to analyze the impact of an individual fuel cell's operating parameters on cell performance. Using this model, it is also possible to determine the activation loss parameters of the PEM fuel cell. The model is well adapted for the PEM cell and incorporates the key physical and electrochemical processes that happen in the cell.

*Corresponding author
Email addresses: abeicha@yahoo.com (Abdellah Beicha*), zaamouche.radia@yahoo.fr (Radia Zaamouche)

2. Experimental

2.1. Electrode preparation

For the electrode preparation, a substrate made from carbon cloth "A" with thickness 350 μm, platinum-supported carbon 10 wt% Pt/C, activated carbon black, and Teflon (PTFE) 60 wt% were used. Two different platinum loadings were used in preparation of the electrodes. One electrode was with platinum loading 0.18 mg Pt/cm^2; while the second was with platinum loading 0.38 mg Pt/cm^2. The composition of the catalyst layer was 70 wt% Pt/C and 30 wt% Teflon (PTFE). Detailed electrode preparation can be found in reference [9].

2.2. Operation of a single cell in fuel cell test apparatus

During the operation of PEM fuel cells, the following processes take place in the electrode: (i) the reactant gases diffuse through the porous backing layer; (ii) at the gas-electrolyte interface, the gases dissolve and then diffuse to the electrolyte-electrode interface; (iii) electro-catalytic reaction inside the catalyst layer precedes the gas adsorption at the electrode surface; (iv) ionic transport occurs in the electrolyte, but electronic transport takes place in the electrode.

Oxygen and hydrogen were passed through humidifiers before being fed into the cell cells. Hydrogen was fed into the anode at a flow rate of 140 ml/min and 1 atm. Oxygen entered the fuel cell through the cathode at a flow rate of 380 ml/min and 2 atm. The electrons generated from the anode were connected to a digital multimeter, with an external variable resistance to measure the current and voltage produced by the cell. Electric conductivity was measured by using a resistivity meter (Loresta-GP MCP-T600). The specific resistance of the gas diffusion layer composed of 70 wt% Pt/C and 30 wt% PTFE was measured to be 0.21 Ω·cm. The parameters of the fuel cells used in the simulation are listed in Table 1.

Table 1: Parameters used in the simulation

Parameters	Value
Temperature, T	298 K
Pressure, P	1 atm
Electrode Area	25 cm^2
Membrane thickness, l_m	117 μm
Diffusion layer thickness, l_d	350 μm
P_{O_2}	2 atm
P_{H_2}	1 atm
Diffusion layer electronic conductivity, σ_d	5 Ω^{-1}cm^{-1}
Diffusion coefficient of H_2 into H_2O, D_{H_2,H_2O}	1.6×10^{-4} m^2/s
Diffusion coefficient of O_2 into H_2O, D_{O_2,H_2O}	3.11×10^{-5} m^2/s
Diffusion coefficient of H2O into membrane, $D_{H_2O,m}$	3×10^{-10} m^2/s
Equivalent weight, EW	1100 g/mol
Dry membrane density, ρ_{dry}	2020 Kg/m^3

3. PEM fuel cell modeling

3.1. Basic fuel cell operation

A PEM fuel cell consists of a membrane through which hydrogen ions diffuse from anode to cathode. A schematic diagram of a PEM fuel cell is shown in Fig. 1.

The hydrogen diffuses through the electrode until it reaches the catalytic layer of the anode where it reacts to form protons and electrons, as shown below in the reaction:

$$H_2 \rightarrow 2H^+ + 2e^- \tag{1}$$

The protons are transferred through the membrane to the catalytic layer of the cathode. Electrons pass through an external electric circuit to the cathode. On the cathode side of the fuel cell, protons, electrons and oxygen react in the following reaction:

$$2H^+ + 2e^- + \frac{1}{2}O_2 \rightarrow H_2O + heat \tag{2}$$

Hence, the overall chemical reaction of the PEM fuel cell is

$$H_2 + \frac{1}{2}O_2 \rightarrow H_2O + heat + energy \tag{3}$$

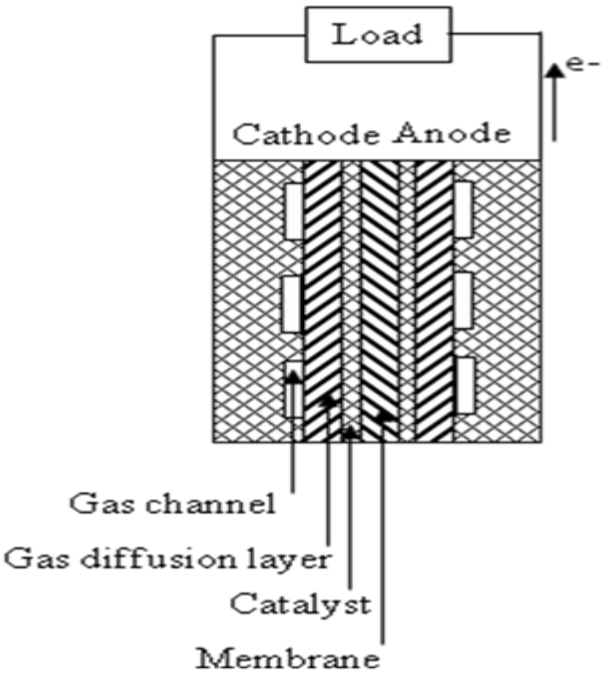

Figure 1: Schematic of a PEM fuel cell

3.2. Model formulation

3.2.1. Electrochemical model

The output voltage of a single cell can be defined as the result of the following [5, 10]:

$$V_{cell} = E - V_{activation} - V_{ohmic} - V_{concentration} \tag{4}$$

In the equation above, E is the thermodynamic potential of the cell and it represents its reversible voltage; $V_{activation}$ is the voltage drop due to the activation of the anode and cathode, a measure of the voltage drop associated with the electrodes; V_{ohmic} is the ohmic voltage drop, a measure of the ohmic voltage drop resulting from the resistances of the conduction of protons through the solid electrolyte and the electrons through its path; and $V_{concentration}$ represents the voltage drop resulting from the reduction in concentration of the reactants gases or, alternatively, from the transport of mass of oxygen and hydrogen; and fuel cell's output power density is given by:

$$P_{cell} = V_{cell} i \tag{5}$$

Each of the terms of Eq. (4) is discussed and modeled separately in the subsections that follow.

Cell reversible voltage. The fuel cell's output voltage is determined by the cell's reversible voltage, which arises from the potential difference produced by the chemical reaction and several voltage losses that take place inside the cell. The fuel cell's reversible voltage is a function of temperature and partial pressures of reactants and product, as is shown in the following equation:

$$\begin{aligned} E = {} & \tfrac{\Delta G}{2F} + \tfrac{\Delta S}{2F}\left(T - T_{ref}\right) + \\ & \tfrac{RT}{2F}\left[\ln\left(P_{H_2}\right) + \tfrac{1}{2}\ln\left(P_{O_2}\right)\right] \end{aligned} \tag{6}$$

where ΔG is the change in the Gibbs free energy; F is the constant of Faraday; ΔS is the change of the entropy; R is the universal constant of the gases; while P_{H_2} and P_{O_2} are the partial pressures of hydrogen and oxygen, respectively. Variable T denotes the cell operation temperature and T_{ref} the reference temperature. Using the standard pressure and temperature (SPT) values for ΔG, ΔS and T_{ref}, Eq. (6) can be simplified to [10]:

$$\begin{aligned} E = {} & 1.229 - 0.85 \times 10^{-3}\left(T - 298.15\right) \\ & +4.31 \times 10^{-5} T\left[\ln\left(P_{H_2}\right) + \tfrac{1}{2}\ln\left(P_{O_2}\right)\right] \end{aligned} \tag{7}$$

Activation voltage drop. Activation polarization is related to the energy barrier that must be overcome to initiate a chemical reaction between reactants. At low current draw, the electron transfer rate is slow and a portion of the electrode voltage is lost in order to compensate for the lack of electro-catalytic activity. Expression for activation losses is given by:

$$V_{activation} = \frac{RT}{2\psi F}\ln\left(\frac{i}{i_0}\right) \tag{8}$$

ψ is electron transfer coefficient, and is unit less. This value describes the proportion of the electrical energy applied that is harnessed in changing the rate of an electrochemical reaction. It is this value that differs from one material to another. i represents the cell's current density, whereas i_0 is exchange current density. i_0 is the value on the Tafel plot when the current begins to move away from zero.

Due to higher anode exchange current density, cathode activation losses are significantly higher so anode activation losses are negligible. The value of

cathode exchange current density also depends on operating parameters, as is shown by:

$$i_{0c} = 2Fk_c \exp\left(\frac{2.46\beta F}{RT}\right) \tag{9}$$

β and k_c are, respectively, symmetry factor and factor related to reaction speed.

Ohmic voltage drop. Ohmic voltage drop (or "Ohmic polarization") occurs due to resistive losses in the cell. These resistive losses occur within the electrolyte (ionic), in the electrodes (electronic and ionic), and in the terminal connections in the cell (electronic). Since the stack plates and electrolyte obey Ohm's law, the amount of voltage lost in order to force conduction varies mostly linearly throughout this region. This is the working region of the fuel cell.

$$V_{ohmic} = i\,(r_{ion} + r_{el}) \tag{10}$$

The following expression for the ionic resistance is used [10]:

$$r_{ion} = l_m \frac{181.6\left[1 + 0.03i + 0.062\left(\frac{T}{303}\right)^2 i^{2.5}\right]}{(\lambda - 0.634 - 3i)\exp\left[4.18\left(\frac{T-303}{T}\right)\right]} \tag{11}$$

where l_m is the thickness of the membrane. The parameter λ is influenced by the membrane preparation [11] and it can be related to relative humidity of the membrane Φ by the following expression [12]:

$$\lambda = 0.043 + 17.8\Phi - 39.8\Phi^2 + 36.0\Phi^3 \tag{12}$$

The electronic resistance can be written as:

$$r_{el} = \frac{2l_d}{\sigma_d} \tag{13}$$

where l_d is diffusion layer thickness and σ_d is diffusion layer electronic conductivity.

Concentration or mass transport voltage drop. Mass transport or concentration polarization results when the electrode reactions are hindered by mass transfer effects. In this region, the reactants become consumed at greater rates than they can be supplied, while the product accumulates at a greater rate than it can be removed. Ultimately, these effects inhibit further reaction altogether and the cell voltage drops to zero. Expression for the fuel cell's concentration losses is given by:

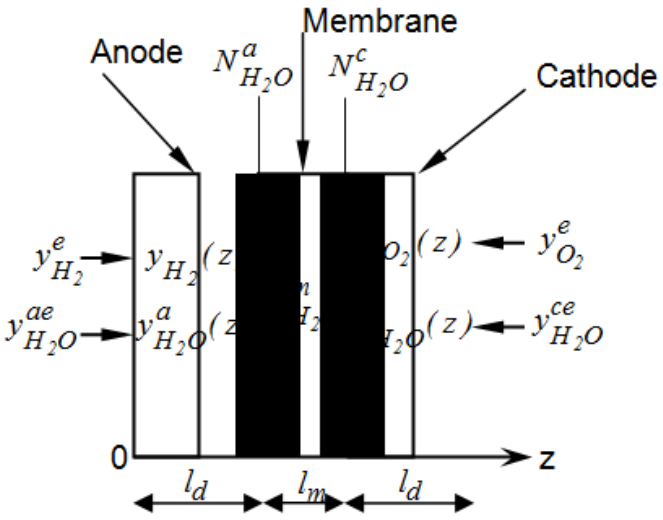

Figure 2: Mass transport through MEA

$$V_{concentration} = -\frac{RT}{2F}\ln\left(1 - \frac{i}{i_L}\right) \tag{14}$$

i_L represents limiting current density. This parameter describes the maximum current density that can flow through the electrode.

3.2.2. Mass transport

Molar flux. At anode channel:

Molar flux of hydrogen,

$$N_{H_2} = \frac{i}{2F} \tag{15}$$

At membrane:

Molar flux of H^+,

$$N_{H^+} = \frac{i}{F} \tag{16}$$

At cathode channel:

Molar flux of oxygen,

$$N_{O_2} = -\frac{i}{4F} \tag{17}$$

At interface membrane-anode:

$$N^{a}_{H_2O} = N^{m}_{H_2O} \tag{18}$$

At interface membrane-cathode:

$$N^{c}_{H_2O} = N^{m}_{H_2O} + N^{prod}_{H_2O} \; and \; N^{prod}_{H_2O} = \frac{i}{2F} \tag{19}$$

Diffusion of species. At anode channel:

$$y_{H_2} + y^{a}_{H_2O} = 1 \tag{20}$$

At cathode channel:

$$y_{O_2} + y^{c}_{H_2O} = 1 \tag{21}$$

The Stefan-Maxwell equation in one dimension can be written as:

At anode channel:

$$\frac{dy_{H_2}}{dz} = \frac{1}{cD_{H_2,H_2O}} \left[y_{H_2} \left(N^{a}_{H_2O} + N_{H_2} \right) - N_{H_2} \right] \tag{22}$$

where $c = \frac{P}{RT}$

Eq. (22) can be solved by using the following boundary conditions:

$$y^{ae}_{H_2O} = RH_a \frac{P_{sat}}{p} \tag{23}$$

$$y^{e}_{H_2} = 1 - y^{ae}_{H_2O} \tag{24}$$

At cathode channel:

$$\frac{dy_{O_2}}{dz} = \frac{1}{cD_{O_2,H_2O}} \left[y_{O_2} \left(N^{c}_{H_2O} + N_{O_2} \right) - N_{O_2} \right] \tag{25}$$

That can be solved by using the following boundary conditions:

$$y^{ce}_{H_2O} = RH_c \frac{P_{sat}}{p} \tag{26}$$

$$y^{e}_{O_2} = 1 - y^{ce}_{H_2O} \tag{27}$$

Membrane transport.

$$c_{H_2O} = \frac{\rho_{dry}\lambda}{EW} \tag{28}$$

$$\Phi = y^{a,c}_{H_2O} \frac{P}{P_{sat}} \tag{29}$$

The vapor pressure is given by

$$\frac{P_{sat}}{P} = \exp\left(13.67 - \frac{5096.23}{T} \right) \tag{30}$$

Water transport in the membrane is given by:

$$N^{m}_{H_2O} = \frac{0.114\lambda i}{F} - D_{H_2O,m} \frac{dc_{H_2O}}{dz} \tag{31}$$

$$\frac{\lambda(z) - \lambda_a}{\lambda_c - \lambda_a} = \frac{1 - \exp(k_m z)}{1 - \exp(k_m l_m)} \tag{32}$$

where

$$k_m = \frac{0.114 \times EW \times i}{\rho_{dry} D_{H_2O,m} F} \tag{33}$$

From Eqs. (28), (31) and (32), one can get $N^{m}_{H_2O}$ as:

$$N^{m}_{H_2O} = \frac{0.114i}{F} \left[\lambda_a + \frac{\lambda_c - \lambda_a}{1 - \exp(k_m l_m)} \right] \tag{34}$$

4. Results and discussions

Concentration polarization results from restrictions on the transport of the fuel gases to the reaction sites. This usually occurs at high current, because the forming of product water and excess humidification blocks the reaction sites. This polarization is also affected by the physical restriction of the transfer of oxygen to the reaction sites on the cathode side of the fuel cell. Concentration polarization can be reduced by using thinner electrodes, which shortens the path of the gas to the sites [13, 14]. Jordan et al. [14] observed a dramatic change in slope of the voltage versus current density plot using air oxidant. This change, indicative of a diffusion-limited reaction, was not so apparent when pure oxygen is used as the oxidant. The same behavior was also observed by other researchers [15]. This is consistent with the experimental data showed in Fig. 2. Hence, in parameter estimation the authors neglected the effect of concentration polarization drop.

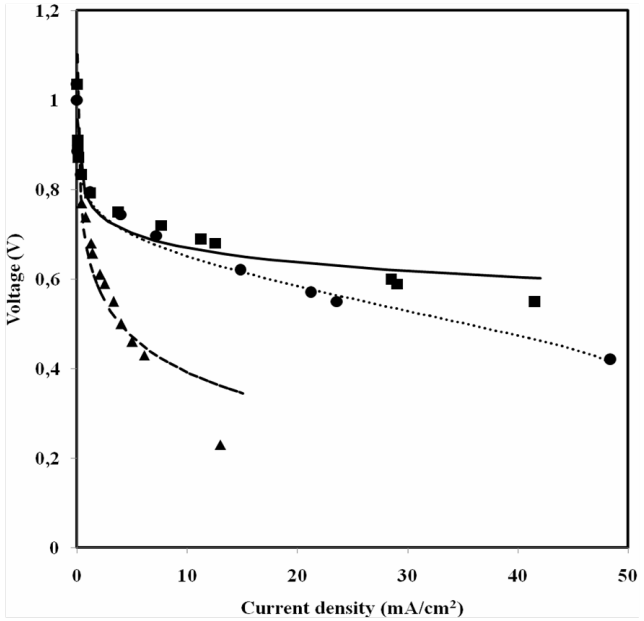

Figure 3: Fuel cell voltage as a function of the cell's current density at T = 298 K, data: ▲ Pt loading = 0.18 mg/cm-2, ■ Pt loading = 0.38 mg/cm^2 and • E-TECK electrode with Pt loading = 0.4 mg/cm^2 [9]; model: (dashed line) Pt loading = 0.18 mg/cm^2, (solid line) Pt loading = 0.38 mg/cm^2 and (dotted line) E-TECK electrode with Pt loading = 0.4 mg/cm^2

Table 2: Variation of the parameters ψ and i_0 with platinum loading at T = 298K

Parameters	Fabricated electrode 0.18 mg Pt/cm^2	Fabricated electrode 0.38 mg Pt/cm^2	E-TECK electrode 0.4 mg Pt/cm^2
ψ	0.13	0.28	0.3
i_0, A/cm^2	2.94×10^{-9}	4.95×10^{-8}	2.86×10^{-8}

4.1. Determination of the activation loss parameters

The experimental data of the cell voltage versus current density (Fig. 3) for the two fabricated electrodes and the commercial electrode E-TECK with Pt loadings 0.18, 0.38 and 0.4 mg/cm^2, respectively, are fitted to the present model using a nonlinear least squares method. The characteristics of fabricated and commercial electrodes are listed in Table 1. The activation loss parameters, and i_0, are determined and listed in Table 2. Both parameters depend on Pt loading. The increase of Pt loading will cause an increase of and i_0. This can be attributed to the increase in active sites for hydrogen adsorption.

An inconsistency is observed between the polarization curves for the prepared electrode with Pt loading 0.38 mg/cm^2 and the commercial on E-TECK with Pt loading 0.4 mg/cm^2. The cell voltage in E-TECK dropped slightly faster than the former electrode. Also, the value of i_0 is decreased from 4.95×10^{-8} A/cm^2 (prepared electrode with Pt loading 0.38 mg/cm^2) to 2.86×10^{-8} A/cm^2 (E-TECK electrode with Pt loading 0.4 mg/cm^2). This may be attributed to the fabrication process in the preparation of electrode with Pt loading 0.38 mg/cm^2, which creates a better particle distribution of electrocatalyst. The placing of platinum in the catalyst layer can be improved through the spraying technique [9]. The estimated values of i_0 are lower than those reported by Amphlett et al. [16], which are 107.6×10^{-8} A/cm^2 at 298 K. From these results, it can be concluded that Pt loading is not alone in affecting the value of i_0.

Typically, the value of lies in a very narrow range of about 0.1 to 0.5 [17]. The exchange current density constant varies over a wide range, and thus has a dramatic effect on the performance of fuel cells at low current densities. Hence, it is vital to design fuel cells with high exchange current densities.

4.2. Effect of temperature on the performance of the PEM fuel cell

Fuel cell voltage as a function of the cell's current density is shown in Fig. 4. In Fig. 5 the cell's power density is shown as a function of current density for two different temperatures. It can be seen from these figures that the fuel cell's efficiency is low and that a significant part of the theoretical output voltage is lost because of various losses inside the cell. Also noticeable is that an increase in fuel cell operating temperature will cause an increase in the cell's output voltage and power. An increase in temperature from 298 K to 353 K gives a 28% increase in fuel cell voltage (Fig. 4). The reason for this is that higher temperatures improve mass transfer within fuel cells and results in a net decrease in cell resistance, thereby improving the reaction rate.

4.3. Effect of the partial pressures

Change in output power related to increase in partial pressures is shown in Fig. 6. It can be seen that the power increase due to reactant pressure increase

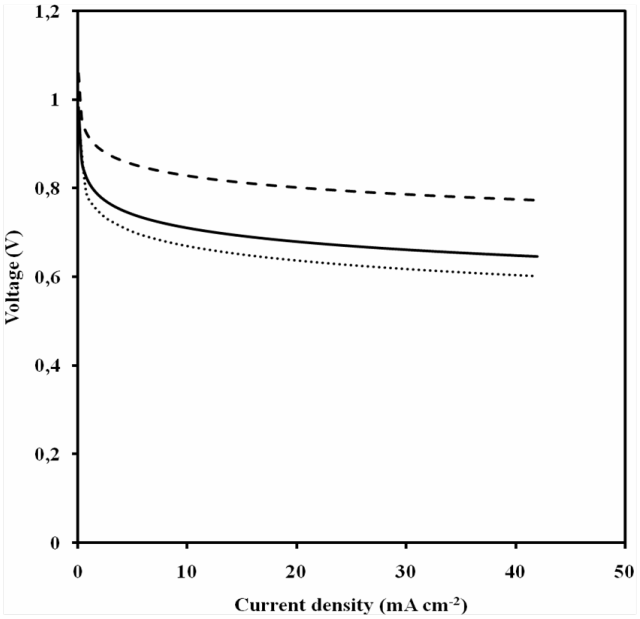

Figure 4: Fuel cell voltage as a function of the cell's current density for various temperatures at Pt loading = 0.38 mg/cm^2; model: (dotted line) 298 K, (solid line) 313 K and (dashed line) 353 K

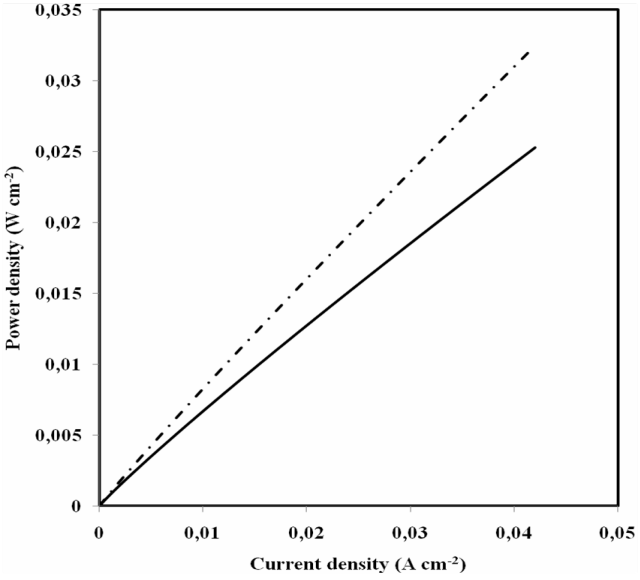

Figure 5: Fuel cell power density as a function of the cell's current density for various temperatures at Pt loading = 0.38 mg/cm^2; model: (solid line) 298 K and (dashed line) 353 K

is 1.1%, which is smaller than the change caused by temperature variations.

4.4. Membrane humidity

Sufficient gas stream humidification is essential for PEM fuel cell operation since water molecules move with the hydrogen ions during the ion exchange reaction. Insufficient humidification water dehydrates the membrane and can lead to cracks or holes in the membrane. A decrease in membrane humidity from 100% to 30% decreases fuel cell voltage by 1.8% (Fig. 7). Reducing membrane humidity can result in slightly slower electrode kinetics, including electrode reaction and mass diffusion rates.

Analysis of the profiles of water content in the membrane can provide some recommendations for the humidification of gases. The profiles of water content in the membrane are given in Fig. 8. This figure shows the influence of transport by electro-osmosis on the humidification of the membrane. With low current densities, the profile of water content in the membrane approaches the linear profile imposed by diffusive flow. In contrast, for high current densities, electro-osmotic flow tends to drag water by convection from the anode towards the cathode.

Description of the mass transport in the electrodes, and in particular in the membrane, is necessary for the modeling of the heat and electron transfer in the fuel cell. Indeed, protonic resistance is strongly dependent on the hydration state of the membrane and this is responsible for a considerable release of heat.

The observed variation of concentrations in the gas mixture on the electrodes shows their weak influence on the transport of water. The variations of the molar fraction of water in the electrodes (anodic and cathodic) are given in Figures 9 and 10. These variations are observed to be more important in the cathodic electrode than in the anodic one. It should be noted that these variations are slightly dependent on the current density.

These simulations show that attention must be paid to temperature, whereas reactant pressures and membrane humidity have a less significant influence on output voltage and power.

5. Conclusion

Using the present PEM fuel cell model, the authors analyzed the influence of fuel cell operating param-

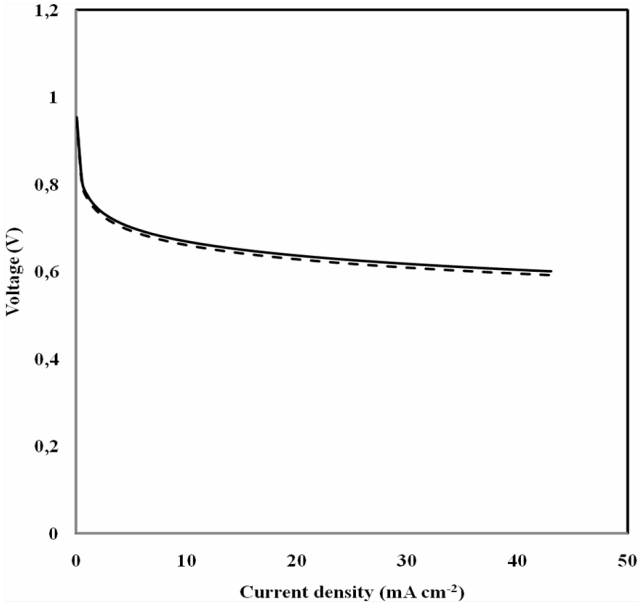

Figure 6: Fuel cell voltage as a function of the cell's current density for various fuel cell reactants partial pressure at T = 298 K and Pt loading = 0.38 mg/cm^2; model: (dashed line) P_{H_2} = 0.995×10^5 Pa and P_{O_2} = 0.606×10^5 Pa, (solid line) P_{H_2} = 1.01×10^5 Pa and P_{O_2} = 1.01×10^5 Pa

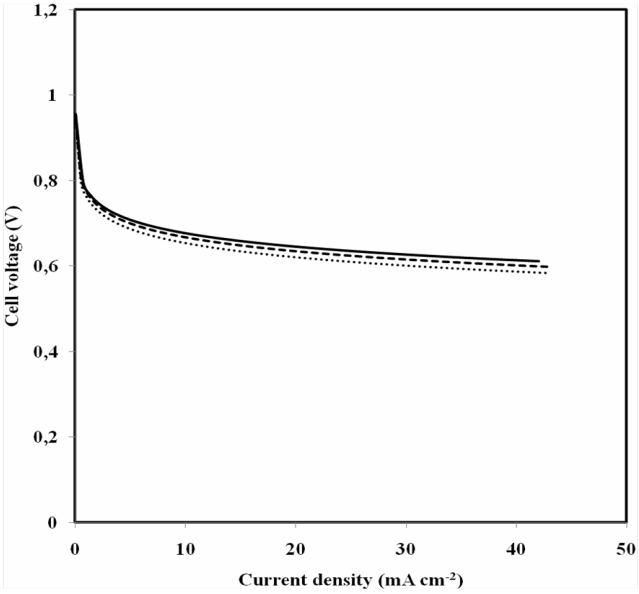

Figure 7: Fuel cell voltage as a function of the cell's current density for various membrane humidity at T = 298 K and Pt loading = 0.38 mg/cm^2; model: (solid line) Φ = 100%, (dashed line) 50% and (dotted line) Φ = 30%

eters (temperature, partial pressures and membrane humidity) on fuel cell performance. Temperature was found to have a significant influence on output voltage and power. The influence of partial pressures and membrane humidity is less significant.

Both the electron transfer coefficient and exchange current density are platinum loading dependent. The exchange current density constant varies significantly with platinum loading and thus has a dramatic effect on fuel cell performance at low current densities. This parameter is crucial for the purpose of PEM fuel cell design.

Acknowledgments

The authors are grateful for financial support from the ministry for higher education and scientific research through national programs of research.

References

[1] R. Cownden, M. Nahon, M. Rosen, Modelling and analysis of a solid polymer fuel cell system for transportation applications, International Journal of Hydrogen Energy 26 (6) (2001) 615–623. doi:10.1016/S0360-3199(00)00126-9.

[2] A. Rowe, X. Li, Mathematical modeling of proton exchange membrane fuel cells, Journal of Power Sources 102 (1–2) (2001) 82–96. doi:10.1016/S0378-7753(01)00798-4.

[3] D. Bevers, M. Wohr, K. Yasuda, K. Oguro, Simulation of a polymer electrolyte fuel cell electrode, Journal of Applied Electrochemistry 27 (1997) 1254–1264. doi:10.1023/A:1018488021355.

[4] G. Maggio, V. Recupero, L. Pino, Modeling polymer electrolyte fuel cells: an innovative approach, Journal of Power Sources 101 (2) (2001) 275–286. doi:10.1016/S0378-7753(01)00758-3.

[5] J. Amphlett, R. Mann, B. Peppley, P. Roberge, A. Rodrigues, A model predicting transient responses of proton exchange membrane fuel cells, Journal of Power Sources 61 (1–2) (1996) 183–188. doi:10.1016/S0378-7753(96)02360-9.

[6] J. Hamelin, K. Agbossou, A. Laperrière, F. Laurencelle, T. Bose, Dynamic behavior of a pem fuel cell stack for stationary applications, International Journal of Hydrogen Energy 26 (6) (2001) 625 – 629. doi:10.1016/S0360-3199(00)00121-X.

[7] H. P. van Bussel, F. G. Koene, R. K. Mallant, Dynamic model of solid polymer fuel cell water management, Journal of Power Sources 71 (1–2) (1998) 218–222. doi:10.1016/S0378-7753(97)02744-4.

[8] Z. Zhang, X. Huang, J. Jiang, B. Wu, An improved dynamic model considering effects of temperature and equivalent internal resistance for pem fuel cell power modules, Journal of Power Sources 161 (2) (2006) 1062–

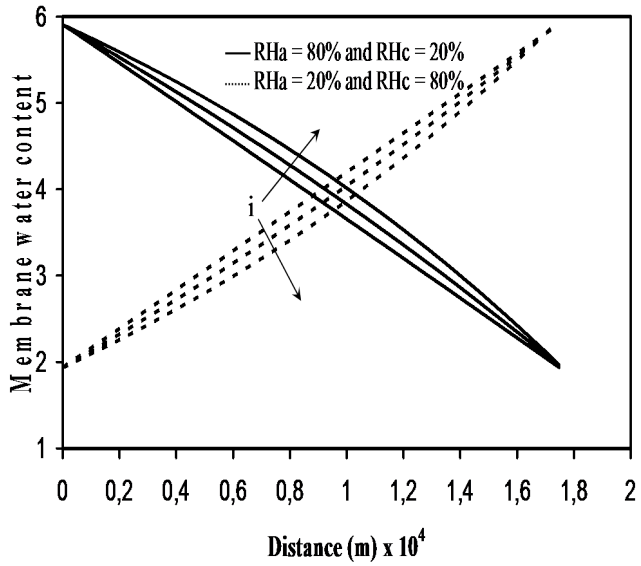

Figure 8: Variation of membrane humidity for i = 0.01; 0.1; 0.2 A/cm^2

1068. doi:10.1016/j.jpowsour.2006.05.030.

[9] R. Chebbi, A. Beicha, W. Daud, R. Zaamouche, Surface analysis for catalyst layer (pt/ptfe/c) and diffusion layer (ptfe/c) for proton exchange membrane fuel cells systems (pemfcs), Applied Surface Science 255 (12) (2009) 6367–6371. doi:10.1016/j.apsusc.2009.02.017.

[10] R. F. Mann, J. C. Amphlett, M. A. Hooper, H. M. Jensen, B. A. Peppley, P. R. Roberge, Development and application of a generalised steady-state electrochemical model for a pem fuel cell, Journal of Power Sources 86 (1–2) (2000) 173–180. doi:10.1016/S0378-7753(99)00484-X.

[11] M. G. Nguyen, R. White, A water and heat management model for proton-exchange-membrane fuel cells, Journal of Electrochemical Society 140 (8) (1993) 2178–2186.

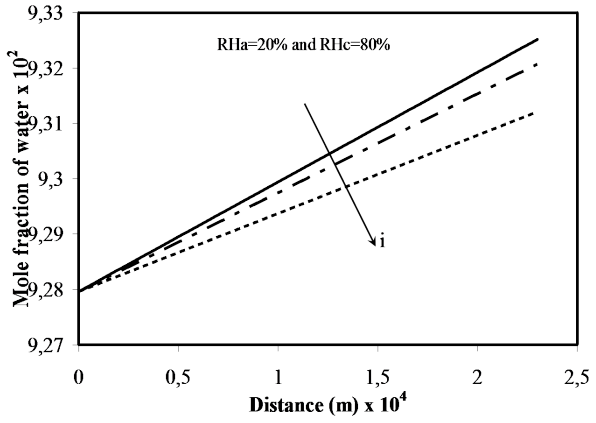

Figure 9: Variation of mole fraction of water at anode for i = 0.01; 0.04; 0.1 A/cm^2

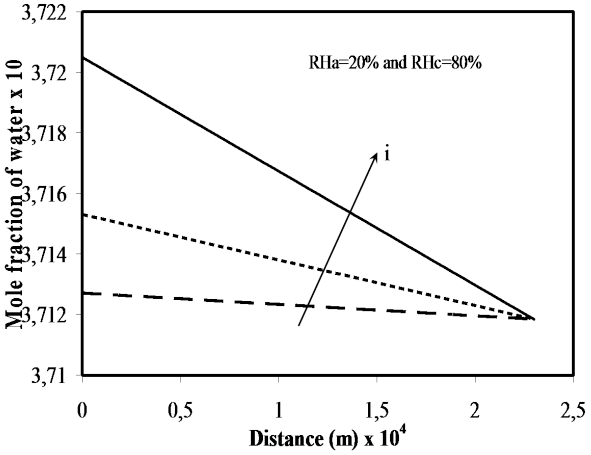

Figure 10: Variation of mole fraction of water at cathode for i = 0.01; 0.04; 0.1 A/cm^2

[12] T. Springer, T. Zawodzinski, S. Gottesfeld, Polymer electrolyte fuel cell model, Journal of Electrochemical Society 138 (8) (1991) 2334–2342.

[13] J. H. Hirschenhofer, Fuel cell status 1994, IEEE AES Systems Magazine (1994) 10–15.

[14] L. Jordan, A. Shukla, T. Behrsing, N. Avery, B. Muddle, M. Forsyth, Diffusion layer parameters influencing optimal fuel cell performance, Journal of Power Sources 86 (1–2) (2000) 250–254. doi:10.1016/S0378-7753(99)00489-9.

[15] J. Song, S. Cha, W. Lee, Optimal composition of polymer electrolyte fuel cell electrodes determined by the ac impedance method, Journal of Power Sources 94 (1) (2001) 78 – 84. doi:10.1016/S0378-7753(00)00629-7.

[16] J. Laminie, A. Dicks, Fuel cell systems explained, 2nd Edition, Wiley & Sons, England, 2005.

[17] J. C. Amphlett, R. M. Baurnet, R. F. Mann, Performance modeling of the ballard mark iv solid polymer electrolyte fuel cell, Journal of Electrochemical Society 142 (1) (1995) 1–15.

Nomenclature

β	symmetry factor
λ	water content
λ_a	water content
λ_c	water content
Φ	relative humidity,
ψ	electron transfer coefficient
ρ_{dry}	dry membrane density, kg/m^3

σ_d diffusion layer electronic conductivity, A/(V·cm)

D_{H_2,H_2O} diffusion coefficient of H_2 in H_2O, m^2/s

$D_{H_2O,m}$ diffusion coefficient of H_2O in membrane, m^2/s

D_{O_2,H_2O} diffusion coefficient of O_2 in H_2O, m^2/s

E fuel cell's reversible voltage, V

EW Equivalent weight, g/mol

F Faraday constant, C

I current density, A/cm^2

i_{0c} cathode exchange current density, A/cm^2

i_0 exchange current density, A/cm^2

i_L limiting current density, A/cm^2

k_c factor related to reaction speed, $A/(cm^2 \cdot C)$

l_d diffusion layer thickness, cm

l_m membrane thickness, cm

N_{H^+} molar flux of H^+, $mol/(m^2 \cdot s)$

$N^a_{H_2O}$ molar flux of H_2O at membrane-anode interface, $mol/(m^2 \cdot s)$

$N^c_{H_2O}$ molar flux of H_2O at membrane-cathode interface, $mol/(m^2 \cdot s)$

$N^m_{H_2O}$ molar flux of H_2O in membrane, $mol/(m^2 \cdot s)$

$N^{prod}_{H_2O}$ molar flux of produced water, $mol/(m^2 \cdot s)$

N_{H_2} molar flux of H_2, $mol/(m^2 \cdot s)$

N_{O_2} molar flux of O_2, $mol/(m^2 \cdot s)$

P_{cell} fuel cell's power density, W/cm^2

P_{H_2} partial pressure of hydrogen, atm

P_{O_2} partial pressure of oxygen, atm

R universal gas constant, 8.314 J/(K·mol)

r_{el} electronic resistance, $\Omega \cdot cm^2$

r_{ion} ionic resistance, $\Omega \cdot cm^2$

RH_a relative humidity of anode

RH_c relative humidity of cathode

T temperature, K

V voltage, V

$V_{activation}$ activation voltage drop, V

$V_{concentration}$ concentration voltage drop, V

V_{ohmic} ohmic voltage drop, V

$y^{ae}_{H_2O}$ mole fraction of H_2O at entrance of anode

$y^a_{H_2O}$ mole fraction of H_2O at anode

$y^{ce}_{H_2O}$ mole fraction of H_2O at entrance of cathode

$y^c_{H_2O}$ mole fraction of H_2O at cathode

y_{H_2} mole fraction of H_2

$y^e_{H_2}$ mole fraction of H_2 at entrance of anode

y_{O_2} mole fraction of O_2

$y^e_{O_2}$ mole fraction of O_2 at entrance of cathode

z position, m